Water Science & Technology

IWA PUBLISHING

Water Science & Technology Vol 87 No 11, 2727 doi: 10.2166/wst.2023.164

Prediction of calcium phosphate generation and behaviors of metals during phosphorus recovery using a modified thermodynamic model

Pengzhe Sui [a,b,*], Fumitake Nishimura [a] and Taira Hidaka [a]

[a] Department of Urban and Environmental Engineering, Kyoto University, Kyoto 615-8540, Japan
[b] Research and Development Center, Swing Corporation, Fujisawa 251-8502, Japan
*Corresponding author. E-mail: suipz2005@gmail.com

PS, 0000-0002-6238-4666

ABSTRACT

In this study, behaviors of metals and their effects on phosphorus recovery by calcium phosphate were investigated by the laboratory and pilot experiments as well as by the modified thermodynamic model. Batch experimental results indicated that the efficiency of phosphorus recovery decreased with the increase in metal content and more than 80% phosphorus can be recovered with a Ca/P molar ratio of 3.0 and a pH of 9.0 for the supernatant of an anaerobic tank in the A/O process with the influent containing a high metal level. The mixture of amorphous calcium phosphate (ACP) and dicalcium phosphate dihydrate (DCPD) was assumed to be the precipitated product with an experimental time of 30 min. A modified thermodynamic model was developed using ACP and DCPD as the precipitated products, and the correction equations were incorporated to simulate the short-term precipitation of calcium phosphate based on the experimental results. From the perspective of maximizing both the efficiency of phosphorus recovery and the quality or purity of the recovered product, the simulation results showed that a pH of 9.0 and a Ca/P molar ratio of 3.0 were the optimized operational condition for phosphorus recovery by calcium phosphate when the influent metal content was at the level of actual municipal sewage.

Key words: calcium phosphate, metal, modified thermodynamic model, phosphorus recovery

HIGHLIGHTS

- With a short reaction time, the main recovery product obtained was not HAP but DCPD and ACP.
- Modified thermodynamic model to simulate the inhibition effect of metals and carbonate.
- Co-precipitation of other metals either pH or molar Ca/P increased.
- Optimized operational conditions: molar Ca/P $= 3.0$ and pH $= 9.0$.
- More than 80% of P was recovered for the anaerobic supernatant containing metals under optimized conditions.

GRAPHICAL ABSTRACT

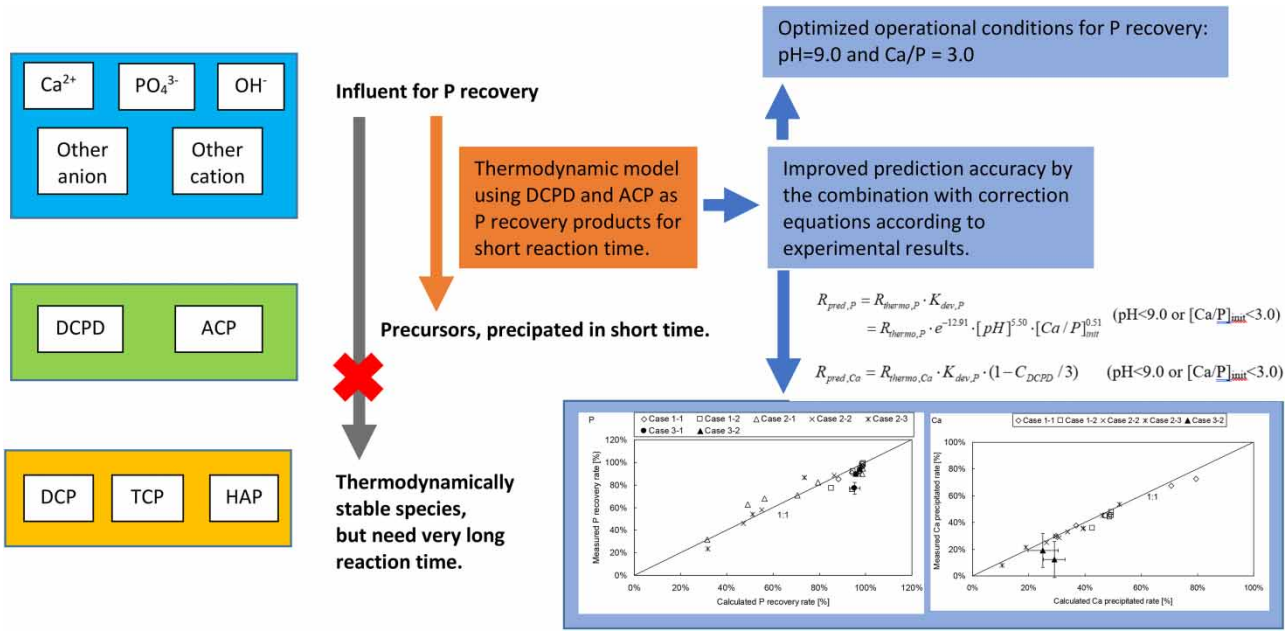

1. INTRODUCTION

Phosphorus is a vital element for humans, animals, and all plants. However, economically exploitable rock resources of phosphate will be depleted in the mid-21st century (Steen 1998; Pindine *et al.* 2021). Most of the phosphate rock is converted into fertilizer, but only 20% of the applied phosphate fertilizer is consumed by plants and animals and a large amount of phosphorus is discharged into natural water bodies (Peng *et al.* 2018b). Phosphorus in sewage and industrial wastewater is not only a kind of nutrient pollutant responsible for serious eutrophication in enclosed water bodies (besides nitrogen) but also a reservoir of phosphorus resources. With a relatively high concentration in fruit and vegetable wastewater (200–400 $mg{\cdot}L^{-1}$), phosphorus can be recovered and reused by the selected adsorbents (Qin *et al.* 2022). To recover phosphorus in human urine (150–250 $mg{\cdot}L^{-1}$) and reject water after sludge dewatering (approximately 150 $mg{\cdot}L^{-1}$), seawater was used as a precipitant to form struvite (Dai *et al.* 2014; Shaddel *et al.* 2020). But with a relatively low concentration (typically 5 $mg{\cdot}L^{-1}$) in sewage, it is difficult to recover directly, although the recovered phosphorus from sewage can satisfy 15–20% of the world's demand for phosphorus (Yuan *et al.* 2012). The pretreatment by the membrane and microbial fuel cells has great potential for phosphorus recovery because of the enrichment of phosphorus (Peng *et al.* 2018a), but other participating ions are also concentrated at the same time, which could have a negative effect on the recovery. It is reported that phosphorus in sewage was recovered by fluidized bed crystallization of vivianite after biofilm enrichment (Zhou *et al.* 2022). By the worldwide application of the enhanced biological phosphorus removal (EBPR) process, phosphorus is transferred to excess sludge. Phosphorus could be recovered from sewage sludge or the ash of incinerated sewage sludge (Cornel & Schaum 2009; Cieślik & Konieczka 2017). Enhanced phosphorus recovery can be carried out using the released phosphorus from sewage sludge with anaerobic-based treatment (Yu *et al.* 2021), thermal (Meng *et al.* 2019), and thermochemical treatment (Galey *et al.* 2022), or using the extracted phosphorus from sewage sludge ash with the wet chemical extraction (Boniardi *et al.* 2021) and the electrodialytic process (Guedes *et al.* 2014). The major challenge for phosphorus recovery from sewage sludge or sewage sludge ash is the higher concentration of metallic ions than that in sewage caused by bio-adsorption of sewage sludge, and the pretreatment with ion-selective nanofiltration could be an effective way to remove multivalent metal cations (Schütte *et al.* 2015). Although the phosphorus recovery from sewage sludge or sewage sludge ash is promising for resource recovery, it costs a lot for waste disposal. It is better to reduce the generation of excess sludge and recover the resource from sewage, not from sewage sludge.

In order to reduce excess sludge generation and recover phosphorus from the sewage simultaneously, a kind of advanced sewage treatment process combined with excess sludge reduction and phosphorus recovery (SRPR process) has been

developed by incorporating a sludge ozonation unit and a phosphorus crystallization unit into an A/O process (Saktaywin *et al.* 2005, 2006; Nagare *et al.* 2008; Tsuno *et al.* 2008) or an A/A/O process (Tsuno *et al.* 2008; Qiang *et al.* 2015). In this advanced SRPR process (Supplementary material, Figure S1), a part of excess sludge (60–80% in this study) was introduced into the sludge ozonation unit, where excess sludge was treated by ozone to decompose cells and obtain soluble organic product and phosphate, and then ozonated sludge (0.67–0.93% of influent in this study) was fed into the A/O process together with influent and untreated return sludge. In the A/O process, phosphate concentration at the end of anaerobic tank reached a relatively high level caused by anaerobic phosphate release and phosphate inflow from raw sewage as well as ozonated sludge. The mixed liquid with relatively high phosphate concentration was partly drawn out of the A/O process at the end of anaerobic tank and separated solid by settlement tank, and then the soluble orthophosphate in the supernatant of anaerobic tank (SAT) in the A/O process, was partly introduced into the phosphorus crystallization unit (P-cry unit) for recovery. Finally, the supernatant of crystallization unit was returned to the aerobic tank of the A/O process. It is one of the advantages of the SRPR process to use SAT for more effective phosphorus recovery because of concentrated phosphorus (typically 20 $mg{\cdot}L^{-1}$, approximately 5 $mg{\cdot}L^{-1}$ from influent, less than 1 $mg{\cdot}L^{-1}$ from ozonated return sludge since its flowrate was less than 1% of raw sewage, and others from anaerobic phosphorus release) but the same level of metallic ions compared to that in raw sewage. If not from SAT, it is reported that the phosphorus in raw sewage could be recovered by 29% from the supernatant of ozonated sludge (Qiang *et al.* 2015). It should be noted that simultaneous chemical precipitation to remove phosphorus with the addition of iron or aluminum salts is not necessary in this SRPR process. Limited by the ammonia concentration in sewage, calcium phosphates, but not struvite, were generated as the product during phosphorus recovery by the addition of calcium ions and pH adjustment.

As for calcium phosphates, hydroxyapatite (HAP) is the most stable species at normal temperature and pressure. However, its formation will reach equilibrium very slowly over a very much longer time (from a minimum of 1 month to a number of years) than any used in the experiments (Ferguson & McCarty 1971; Musvoto *et al.* 2000a; Celen *et al.* 2007; Cao & Harris 2008). In the actual experimental period (30 min in this study), HAP cannot be the main product although many researchers reported as listed in Table 3 by Peng *et al.* (2018a). In this paper, the possible composition of generated calcium phosphates was discussed based on both thermodynamic considerations and experimental results.

Furthermore, in the P-cry unit of the advanced SRPR process, some may co-precipitate with calcium phosphates, which both decrease the purity of the recovered phosphorus product and affect the accumulation of metals in the advanced sewage treatment process. However, only a few studies have focused on both metals and phosphorus with the objectives of maximizing both P crystal production and their quality (Guney *et al.* 2008; Keller *et al.* 2022). In this study, the behavior of metals during phosphorus recovery was examined, and the improvement of not only the phosphorus recovery rate but also its quality was studied by optimizing operational conditions without an additional separation process. For this purpose, the behaviors of K, Mg, Ca, Al, Fe, Cr, Mn, Ni, Cu, Zn, and Ba were investigated with the measured results in batch and continuous experiments as well as thermodynamic simulation.

In this study, phosphorus recovery by calcium phosphates was investigated by both the laboratory and pilot experiments and a thermodynamic model for the advanced SRPR process. As the thermodynamic model predicts the final equilibrium state, it was modified to be applied to the short-term precipitation for actually used cases. Phosphorus recovery and the behavior of metals are discussed using the modified thermodynamic model under operational conditions of pH ranging from 8.0 to 10.0 and molar ratio of Ca/P ranging from 1.67 to 5. The optimized operational conditions were finally obtained which maximized both phosphorus recovery efficiency and quality of the recovered product (minimum of metals co-precipitation).

2. THERMODYNAMIC MODELING OF CALCIUM PHOSPHATE GENERATION

Thermodynamic modeling is very helpful for understanding the formation of calcium phosphates and their competition with other precipitates, and has been adopted as a powerful tool by many researchers, even though it cannot explain reaction kinetics. Phosphorus crystallization of HAP (Song *et al.* 2002b) and magnesium ammonium phosphate MAP, (Wang *et al.* 2006; Song *et al.* 2015) was investigated using PHREEQC, a fully developed thermodynamic software. Phosphorus recovery by ferric phosphate precipitation from wastewater was examined by PHREEQC and an additional case study (Zhang *et al.* 2010). Phosphate behavior and the fate of counter ions during hydrothermal carbonization of sewage sludge were investigated by thermodynamic model (Ovsyannikova *et al.* 2019). Celen *et al.* (2007) used Visual MINTEQ, a chemical equilibrium model, to predict amendments required to precipitate phosphorus as struvite in liquid swine manure. Phosphorus

recovery by MAP from digested sewage sludge using raw seawater (Shaddel *et al.* 2020) and magnesium salts (Keller *et al.* 2022) as magnesium source was investigated with thermodynamic models to prevent the co-precipitation of heavy metal ions.

Seven crystalline species of calcium phosphates could precipitate during phosphorus recovery, and their reaction pathway is shown in Figure 1. HAP is the most thermodynamically stable species at normal temperature and pressure (Maurer *et al.* 1999; Musvoto *et al.* 2000a). Amorphous calcium phosphate (ACP), octacalcium phosphate (OCP), and dicalcium phosphate dihydrate (DCPD) could act as precursors of HAP (Musvoto *et al.* 2000a). OCP is formed by the hydrolysis of DCPD (Celen *et al.* 2007), while DCPD and ACP are the phases that precipitate firstly – with DCPD precipitating at low pH and ACP at high pH (Musvoto *et al.* 2000a) - and then convert to DCP, tricalcium phosphate (TCP), and HAP as the more thermodynamically stable species (Musvoto *et al.* 2000a). The generation of OCP was reported to be strongly inhibited by the presence of magnesium (Salimi *et al.* 1985) and was not considered in this study. Hydroxypropyl distarch phosphate (HDP) was also not considered since it is reported as a surface complex (Rootare *et al.* 1962; Maurer *et al.* 1999) and no evidence showed its involvement in phosphorus crystallization.

As the initially formed metastable precursors, the generation of the first class of the species (DCPD and ACP) is reported to be a relatively fast process (Musvoto *et al.* 2000a), while the growth of the second class (the more thermodynamically stable

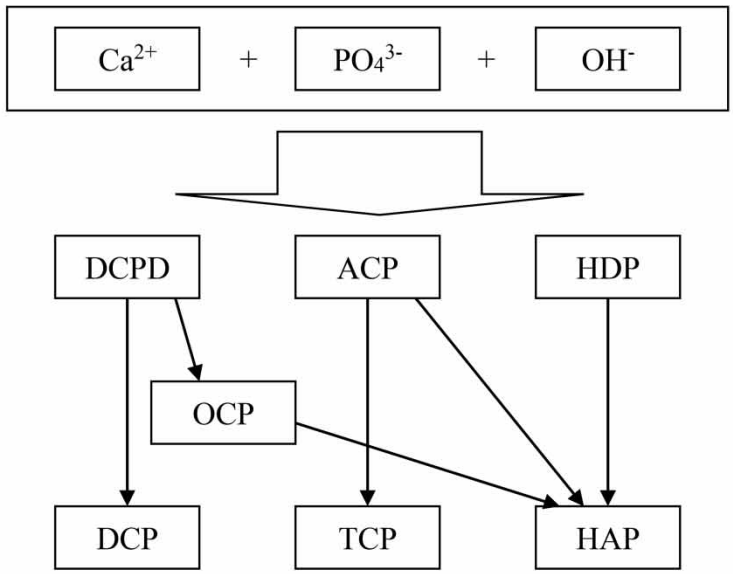

Mineral	Full name	Formula	Ca/P	p*Ks*
HAP	Hydroxyapatite	$Ca_5(PO_4)_3OH$	1.67	48.6[a], 57.5[c]
TCP	Tricalcium phosphate	$Ca_3(PO_4)_2$	1.5	32.7[c], 32.63[c]
DCP	Dicalcium phosphate	$CaHPO_4$	1.0	19.3[c]
ACP	Amorphous calcium phosphate	$Ca_3(PO_4)_2{\cdot}xH_2O$	1.5	26.52[a], 25.46[c], 25.2[c]
OCP	Octacalcium phosphate	$Ca_8(HPO_4)_2(PO_4)_4{\cdot}5H_2O$	1.33	46.9[a]
DCPD	Dicalcium phosphate dihydrate	$CaHPO_4{\cdot}2H_2O$	1.0	6.6[a, c]
HDP	Hydroxydicalcium phosphate	$Ca_2HPO_4(OH)_2$	2.0	27.3[b]

[a]Barat et al. (2008); [b]Maurer et al. (1999); [c]Musvoto et al. (2000a);

Figure 1 | Reaction pathway of calcium phosphate reported in the literature.

species of DCP, TCP or HAP) takes a much longer time – from a minimum of one month to a number of years (Ferguson & McCarty 1971; Musvoto *et al.* 2000a; Celen *et al.* 2007; Cao & Harris 2008).

Without consideration of reaction kinetics, the actual products and composition of calcium phosphates, generated in the operation time range (30 min in this study) during phosphorus recovery, were not able to be predicted by thermodynamic calculation only. However, if the generation of the first class (DCPD and ACP) is fast enough to reach the metastable state in the above reaction time, this metastable state can be predicted by thermodynamic calculation without consideration of the second class (DCP, TCP, and HAP), since its growth is very slow and only generates a very small fraction as discussed above.

Generation reactions of DCPD and ACP are shown in Equations (1) and (2).

$$\text{DCPD generation:} \quad Ca^{2+} + HPO_4^{2-} + 2H_2O \Leftrightarrow CaHPO_4 \cdot 2H_2O \tag{1}$$

$$\text{ACP generation:} \quad 3Ca^{2+} + 2PO_4^{3-} + xH_2O \Leftrightarrow Ca_3(PO_4)_2 \cdot xH_2O \tag{2}$$

Furthermore, it should also be considered that DCPD and ACP generation does not reach full equilibrium under a low pH and a low Ca/P molar ratio for precipitation in as short a period as 30 min. Thus, a correction equation was incorporated based on the experimental results in this study.

Besides calcium phosphates, other important precipitates are calcium carbonates and magnesium carbonates since carbonate could compete with phosphate for calcium ions. Several kinds of minerals are related to calcium carbonates and magnesium carbonates. These include aragonite ($CaCO_3$), calcite ($CaCO_3$), vaterite ($CaCO_3$), dolomite [$CaMg(CO_3)_2$], huntite [$CaMg_3(CO_3)_4$], and magnesite ($MgCO_3$). It has been reported that the presence of Mg^{2+}, phosphate, and dissolved organics decreased the precipitation rate of $CaCO_3$ (Meyer 1984; Musvoto *et al.* 2000b; Celen *et al.* 2007) and that dolomite also exhibited a slow precipitation rate (Mamais *et al.* 1994; Celen *et al.* 2007). No more than a tiny fraction of these two kinds of precipitate could generate in a reaction time of only 30 min and they were not considered in this study, while huntite and magnesite were included during thermodynamic modeling.

3. EXPERIMENTAL INVESTIGATION

3.1. Materials and methods

In this study, precipitation experiments of both batch tests (case 1 and case 2) and continuous operations of a pilot-scale reactor of the advanced SRPR process (case 3) were carried out to investigate the phosphorus recovery by calcium phosphates. The corresponding experimental conditions in the three cases are listed in Table 1. In case 1, the test water was prepared by ultrapure water (UPW) and contained only calcium ions and phosphates. In case 2 and case 3, supernatant from the outflow of the anaerobic tank (SAT) in A/O process (Supplementary material, Figure S1) was employed as the source water. A pilot-scale sequencing batch reactor (SBR) was run as an A/O process using artificial sewage, which only contained essential metals for microorganism growth (Saktaywin *et al.* 2005) in cases 2-1 and 3-1 (low metal level), while containing typical metal composition similar to actual sewage (Asai *et al.* 2005) in cases 2-2, 2-3, and 3-2 (high metal level).

Table 1 | Experimental conditions

Case	Tested water	Metal level	pH	Ca/P	Mode	Determined items
Case 1-1	UPW + Ca + P	Only Ca	9.0	1.67–5	Batch	Soluble P and Ca
Case 1-2	UPW + Ca + P	Only Ca	8–10	3	Batch	Soluble P and Ca
Case 2-1	SAT	Low	8.5–10	1.7–3.4	Batch	Soluble P only
Case 2-2	SAT	High	9.0	1.67–5	Batch	Soluble P and metals
Case 2-3	SAT	High	8–10	3	Batch	Soluble P and metals
Case 3-1	SAT	Low	8.3–9.1	2.7–3.3	Cont.	Soluble P only
Case 3-2	SAT	High	9.0–9.5	3–5	Cont.	Soluble P and metals

UPW, ultrapure water; SAT, supernatant of anaerobic tank; Cont., continuous operational mode.

In all batch tests, phosphate was fixed at 20 mg-P·L^{-1} as the designed inlet concentration of phosphorus to the recovery unit. The different molar ratio of Ca/P was obtained by the adjustment of the calcium concentration, while pH was adjusted by the addition of 1-N NaOH. Besides the batch tests, continuous operation of the advanced SRPR process (Supplementary material, Figure S1) was carried out for about 2.5 months in case 3-1 and 7 months in case 3-2 with two sub-phases (phase 2 and phase 3). More details of the material and methods of experiments are shown in the first part of the Supplementary material.

3.2. Results and discussion

3.2.1. Phosphorus recovery by calcium phosphates in batch tests

All batch experimental results showed that the precipitation of calcium phosphates reached a maximum value in about 1 min (Supplementary material, Figure S2), which indicated that the generation of the first class of calcium phosphates (DCPD and ACP) is fast enough to reach the metastable state in 30 min. As shown in Figure 2(a), more than 80% phosphorus can be recovered in all runs in case 1 for the source water without other metals contained (UPW + Ca + P only), while only about 60% for SAT with low metal content in case 2-1 (Ca/P = 1.7, pH = 9.0), and only about 40% for SAT with high metal content in case 2-2 (Ca/P = 1.7, pH = 9.0). The results indicated that the efficiency of phosphorus recovery decreased with the increase in metal content in the inflow, which was caused by the inhibition effect of metals on the generation of calcium phosphates. Figures 2(b) and 2(c) show the phosphorus recovery efficiency under different initial molar Ca/P ratios and pH values, respectively. Recovered phosphorus was not more than 60% under the condition of a Ca/P molar ratio of no more than 2.0 and a pH of 9.0, or the condition of a Ca/P of 3.0 and a pH of no more than 8.5 for SAT containing high metals level. Correspondingly, more than 80% phosphorus could be recovered with a Ca/P molar ratio of 3.0 and a pH of 9.0, which should be the essential conditions for effective phosphorus recovery for an SAT containing a high metal level.

3.2.2. The behavior of metals in batch tests

The precipitated metal ratios and recovered phosphorus ratio in batch tests of cases 2-2 and 2-3 are shown in Figure 3, which shows that more than 80% of aluminum, manganese, and zinc, and around 60% of chrome transferred to the recovered product (solid phase) in all tests. Most of the barium, copper, magnesium, and potassium remained in the soluble form after batch tests. Iron displayed a different behavior in two groups of batch tests. The precipitated iron ratio decreased from about 40 to 0% when the molar ratio of Ca/P increased from 1.67 to 5, while it increased from 0 to 15% when pH increased from 8.0 to 10.0. The results indicated that the increased molar ratio of Ca/P enhanced the precipitation of calcium phosphates, which led to less phosphate reacting with iron under pH of 9. Furthermore, the increased pH enhanced the precipitation of iron phosphates. The precipitated nickel ratio increased from 24 to 30% and 20 to 35% with respective increases in the molar ratio of Ca/P and pH. The precipitated calcium fluctuated around 30% even if the initial soluble calcium increased from 43.1 mg-Ca·L^{-1} to 129.4 mg-Ca·L^{-1}, and the corresponding molar ratio of Ca/P increased from 1.67 to 5. With a fixed Ca/P molar ratio of 3.0, precipitated calcium increased from 8 to 54% when pH increased from 8.0 to 10.0.

3.2.3. Phosphorus recovery and behavior of metals in continuous experiments

Besides the above batch investigation, the continuous operations of the advanced SRPR process were carried out with two kinds of artificial sewage, which resulted in relatively low and high metals content in the SAT, i.e., the inflow to the P-cry unit, for cases 3-1 and 3-2, respectively.

The phosphorus recovery rate in continuous experiments using an SAT with low metals content (case 3-1) was 77.1 ± 5.3% under pH of 8.3–9.1 and a Ca/P molar ratio of 2.6–3.3, which was almost the same as that of the batch test.

As for the experimental results of continuous operation using an SAT with high metal content in case 3-2, phosphate was shown to recover more than 90% under pH of 9.0–9.5 and a Ca/P molar ratio of 3–5 (Supplementary material, Figure S3(a)). Higher Ca/P molar ratio and pH in case 3-2 than that in case 3-1 contribute to higher phosphorus recovery rate. In comparison with batch tests under a pH of 9.0 and a Ca/P molar ratio of 4.0, the results of phosphorus recovery and co-precipitation of metals in continuous experiments were in accordance with those in the batch test for phosphorus and most metals, but not for barium, copper, iron, and aluminum (Supplementary material, Figure S3(b)). The bio-adsorption of sewage sludge was assumed to contribute to the removal of barium, copper, iron, and aluminum since batch experiments were carried out with filtrated SAT, while pilot continuous experiments with settled SAT, which contained suspended solids of activated sludge.

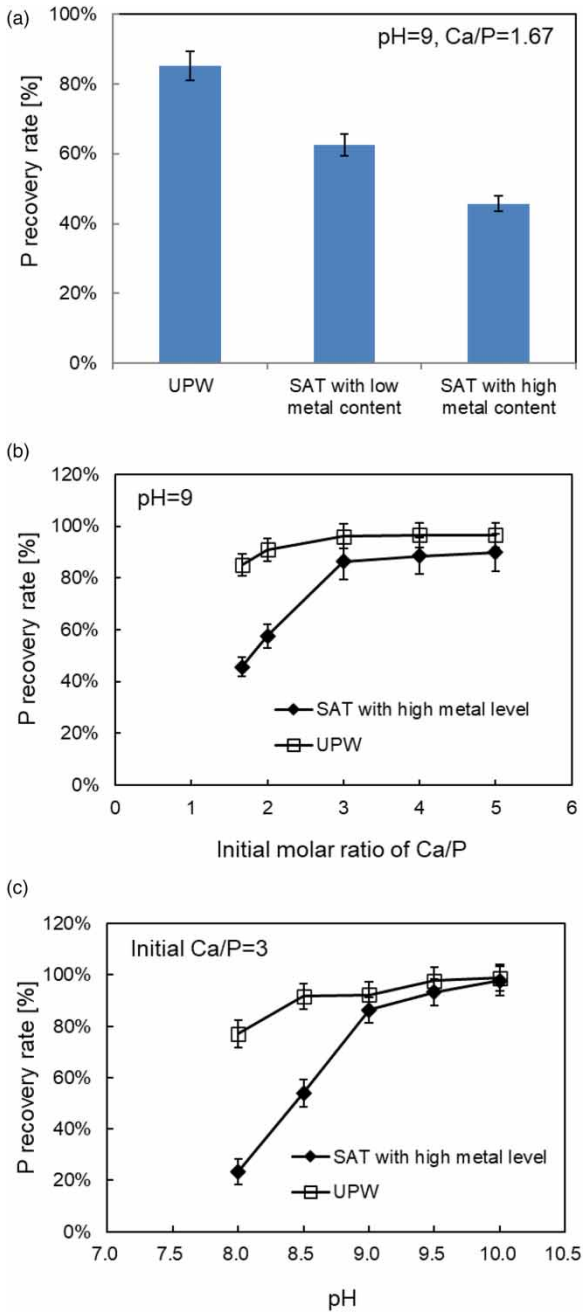

Figure 2 | Phosphorus recovery rate during batch tests ($n = 3$). (a) Different metal contents in the inflow; (b) different initial molar Ca/P; and (c) different pH values.

4. SIMULATION WITH THE THERMODYNAMIC MODEL

4.1. Calculation conditions of the thermodynamic model

As discussed above, the generation of the first class of calcium phosphates (DCPD or ACP) was considered during thermodynamic modeling, and their generation reactions were shown in Equations (1) and (2), respectively. Their corresponding solubility products, reported in the literature, are shown in Figure 1.

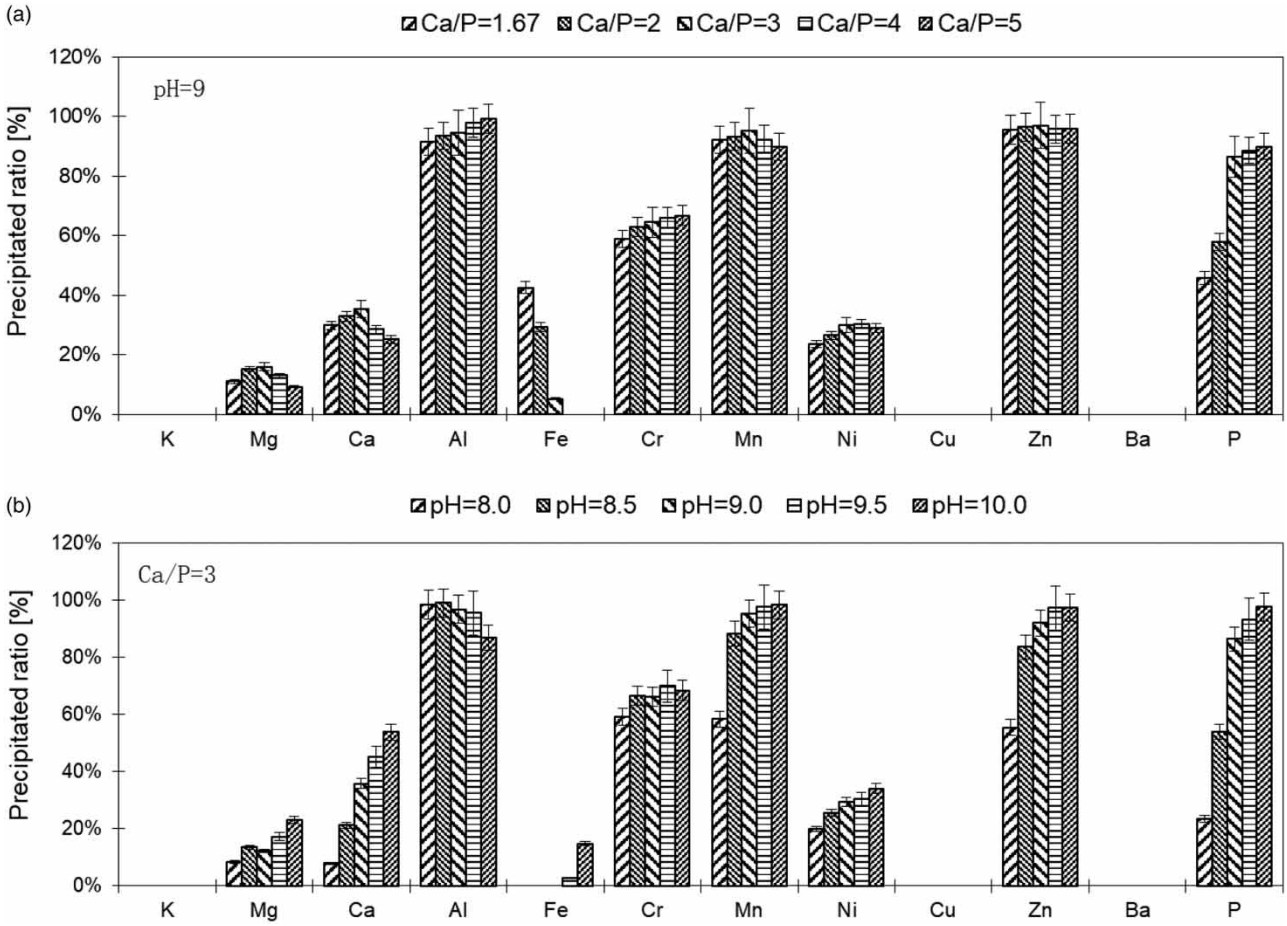

Figure 3 | P recovery ratio and precipitated metal ratio in batch tests under different molar ratios of Ca/P in case 2-2 (a) and different pH values in case 2-3 (b) ($n = 3$).

During thermodynamic modeling of phosphorus recovery, the following aspects need to be considered: (1) all precipitated solids besides the above calcium phosphates and calcium carbonates; (2) all soluble species, such as H^+, OH^-, H_2O, H_3PO_4, $H_2PO_4^-$, HPO_4^{2-}, PO_4^{3-}, H_2CO_3, HCO_3^-, CO_3^{2-}, NH_3, NH_4^+, and all metallic ions; (3) the equilibrium equations of all soluble and precipitated species mentioned above, the mass balance of all elements, and the charge balance of solution; and (4) the effects of temperature, activity, and alkalinity.

In this study, the fully developed free software, Visual MINTEQ (Allison *et al.* 1991), was employed as a tool for thermodynamic calculation. All the factors mentioned above were dealt with by the software, except for the modification of the database to exclude the species with a slow generation rate (HAP, TCP, DCP, OCP, all $CaCO_3$, and dolomite). ACP was not originally included in the database of Visual MINTEQ (version 3.0 and released in April 2010) but was added to the database with the solubility product constant ($pK_s = 26.52$) and the molar ratio of calcium and phosphate (Barat *et al.* 2008).

In batch experiments, it was found that all measured molar ratios of Ca/P in the precipitates were in the range of 1.0–1.5, which was lower than 1.67 (molar Ca/P in HAP). The lower molar ratio of Ca/P indicated HAP was not the main component in generated calcium phosphates with a reaction time of 30 min as discussed above, while the mixture of ACP (Ca/P = 1.5) and DCPD (Ca/P = 1.0) had a high possibility of being the precipitated product. If only ACP and DCPD were contained in the recovery product, in case 1, their generation amounts and ratios in the product were calculated by actual measured calcium and phosphate according to the mass balance of Ca and P. Corresponding calculations can be carried out in cases 2-2 and 2-3 after considering the co-precipitation of calcium by carbonate. It is confirmed that magnesium precipitated only with carbonate by huntite and magnesite according to thermodynamic calculation results. Thus, precipitated calcium by carbonate could be obtained from the measured magnesium precipitation amount and the molar ratio of Ca/Mg in precipitates according to thermodynamic calculation results.

4.2. Modification and verification of the thermodynamic model

4.2.1. The composition of calcium phosphates in recovered product

The possible generated DCPD and ACP percentages in recovered products are shown in Figure 4. It was found that the molar ratio of Ca/P in the precipitates rose with an increase in the initial molar ratio of Ca/P or pH. Correspondingly, the ACP ratio in the recovered product increased while the DCPD decreased. Furthermore, under the condition of a lower Ca/P molar ratio (1.67 in Figure 4(a)) or a lower pH (8.0 in Figure 4(b)), less than 10% of ACP was generated in case of the existence of other metallic ions and carbonates (cases 2-2 or 2-3); while 50–60% of ACP was generated in case of the absence of other metallic ions and carbonates (cases 1-1 or 1-2). These results can be explained by the inhibition effect of other metallic ions and carbonate on ACP generation and are in accordance with reported DCPD/ACP generation, i.e., DCPD precipitating at low pH and ACP at high pH (Musvoto *et al.* 2000a).

4.2.2. Precipitated Ca and P

Comparisons between the results of measured and calculated rates by the thermodynamic model for recovered phosphorus and precipitated calcium in all cases are shown in Figure 5(a) and 5(b), respectively. Figure 5(a) shows that calculated results of phosphorus were in accordance with measured ones in case 1 (with absence of other metals and carbonate) and when pH $\geq$ 9.0 and molar Ca/P $\geq$ 3.0 in case 2 (the SAT containing other metals and carbonate were employed as inflows). However, when pH $<$ 9.0 or molar Ca/P $<$ 3.0 in case 2, the measured phosphorus recovery rates were lower than calculated ones, and the differences ranged from 10 to 55.9%. Under these conditions, the phosphorus recovery rate was lower than 80% in case 2-1 (low metal level, see Supplementary material, Figures S2(e) and S2(f)) or 60% in cases 2-2 and 2-3 (high metal level, see Supplementary material, Figures S2(g) and S2(h)). Furthermore, with enhancement of operational conditions (pH or Ca/P), phosphorus recovery rate increased (Supplementary material, Figure S2), and the difference between measured results and calculated ones decreased at the same time (Figure 5).

The difference between case 1 and case 2 was that the tested water contained metals and carbonate in case 2, but not in case 1. Thus, low measured results resulted from the inhibition effect of metallic ion (Salimi *et al.* 1985) or that of carbonate (Seckler *et al.* 1996; Battistoni *et al.* 1997; Jang & Kang 2002; Song *et al.* 2002a) on the generation of calcium phosphates under the operational conditions of lower pH or smaller molar Ca/P. This also confirmed that the essential operational conditions for SAT were pH of 9.0 and molar Ca/P of 3.0. To correct the deviation between calculated results and measured ones, the multi-regression between the deviation degree (expressed as measured/calculated) and pH together with the initial molar Ca/P was carried out in case 2 with the data of pH $<$ 9 or Ca/P $<$ 3, since the only difference in experimental conditions was pH and the initial Ca/P in each case, and regression results showed the best fit with the expression as follows.

$$K_{dev,P} = \frac{R_{mea,P}}{R_{thermo,P}} = a \cdot [pH]^b \cdot [Ca/P]^c_{init} \tag{3}$$

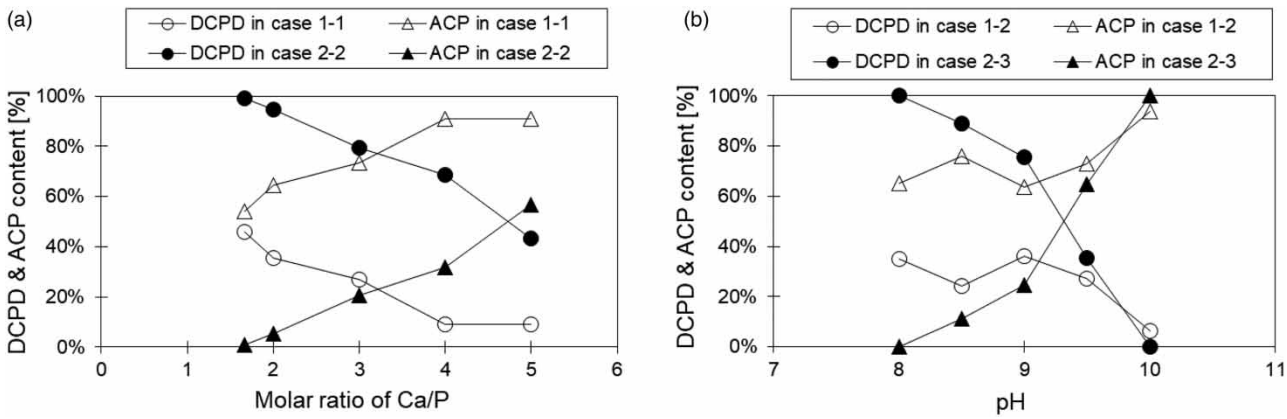

Figure 4 | Possible DCPD and ACP in recovered product according to measured Ca and P content under different initial molar ratios of Ca/P (a) and pH values (b). (Thermodynamic model excludes the species with a slow generation rate: HAP, TCP, DCP, OCP, all $CaCO_3$, and dolomite; and possible DCPD and ACP content was calculated by the molar ratio of precipitated Ca and P.)

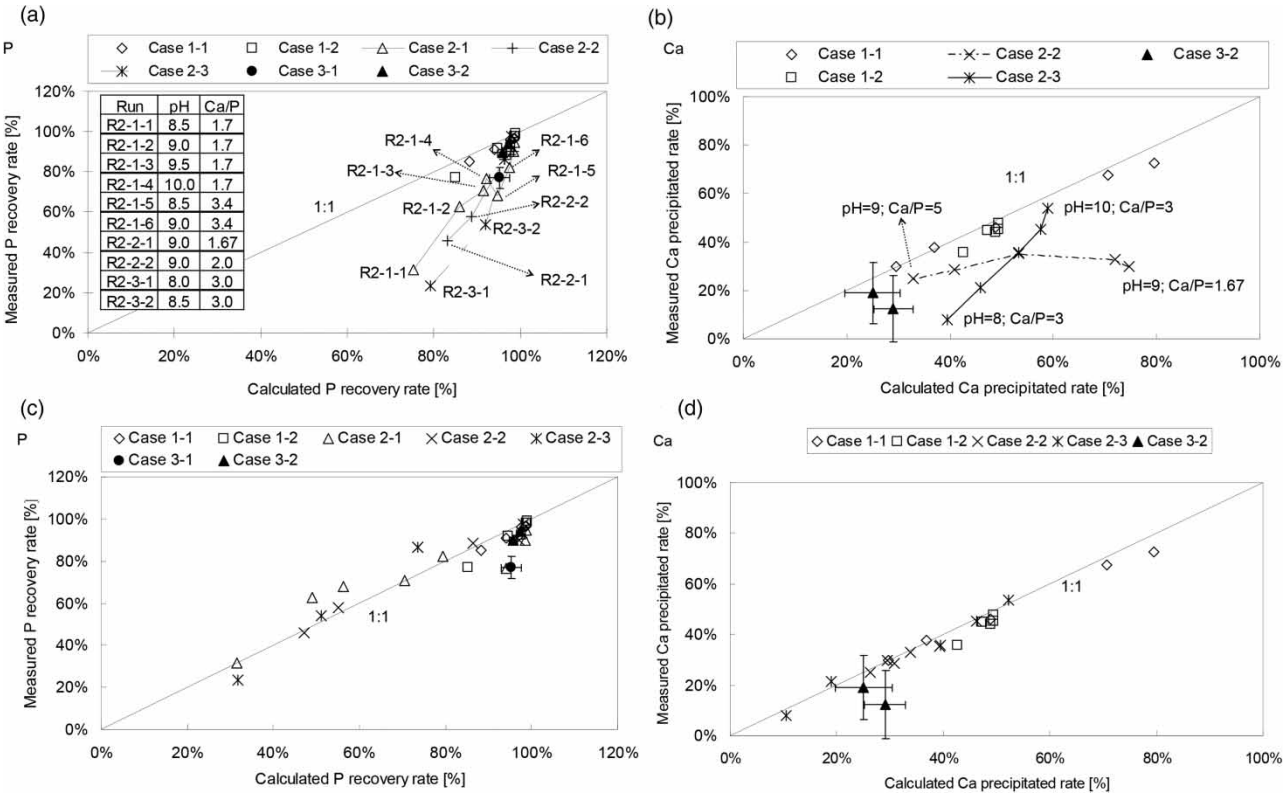

Figure 5 | (a) Comparison between calculated and measured results for precipitated Ca and P; (b) precipitated P and Ca with thermodynamic calculation (without correction); (c) and (d) precipitated P and Ca after correction.

where a, b, c are constants; $[Ca/P]_{init}$ indicates initial molar ratio of Ca/P; $K_{dev,P}$ refers to the deviation degree of P recovery rate between calculated result by thermodynamic model ($R_{thermo,\ P}$) and measured one ($R_{mea,\ P}$).

The regression result is shown in Equation (4) with R^2 of 0.735 for deviation degree of P recovery rate ($K_{dev,P}$).

$$K_{dev,P} = e^{-12.91} \cdot [pH]^{5.50} \cdot [Ca/P]_{init}^{0.51} \quad (\mathrm{pH} < 9.0 \text{ or } [\mathrm{Ca/P}]_{\mathrm{init}} < 3.0) \tag{4}$$

From Equation (4), the final predicted P recovery rate ($R_{pred,\ P}$, should equal to $R_{mea,\ P}$) can be obtained by the following correction equation:

$$\begin{aligned} R_{pred,P} &= R_{thermo,P} \cdot K_{dev,P} \\ &= R_{thermo,P} \cdot e^{-12.91} \cdot [pH]^{5.50} \cdot [Ca/P]_{init}^{0.51} \quad (\mathrm{pH} < 9.0 \text{ or } [\mathrm{Ca/P}]_{\mathrm{init}} < 3.0) \end{aligned} \tag{5}$$

The comparison of the measured P recovery rate and the calculated one, after correction by Equation (5), is shown in Figure 5(c), which indicates that calculated results accorded well with measured ones after correction ($R^2 = 0.900$ for P recovery rate).

Similarly, precipitated ratios of calcium in the calculation results were higher than that of the measured results with low pH or low molar Ca/P as shown in Figure 5(b), which resulted from two mechanisms. Firstly, the precipitated Ca amount should be decreased in accordance with the decrease of the precipitated phosphate amount because of inhibition effects as mentioned above. Secondly, the recovered product in the calculation results by the thermodynamic model was ACP only. Thus, the actual composition of calcium phosphates in the recovered product (the ratio between DCPD and ACP) affected the precipitated calcium ratio, since the molar ratio of Ca/P in DCPD and ACP was different, being 1.0 and 1.5, respectively. The high actual DCPD content in the recovered product resulted in the lower precipitated calcium ratio. To correct the

prediction results of calcium precipitation, the precipitated ratio of calcium by thermodynamic calculation was corrected by considering the decrease of generated calcium phosphates as shown in Equation (5) and the actual composition of DCPD and ACP in the recovered product as shown in the following equation.

$$R_{pred,Ca} = R_{thermo,Ca} \cdot K_{dev,P} \cdot (1 - C_{DCPD}/3) \quad (\mathrm{pH} < 9.0 \text{ or } [\mathrm{Ca/P}]_{\mathrm{init}} < 3.0) \tag{6}$$

where $R_{pred,\ Ca}$ refers to the predicted Ca precipitation ratio after correction; $R_{thermo,\ Ca}$ refers to the Ca precipitation ratio calculated by the thermodynamic model; C_{DCPD} refers to the DCPD ratio in the actual recovery product.

The final predicted ratio of calcium in the precipitates with correction of the thermodynamic calculation by Equation (6) was compared to the measured results as shown in Figure 5(d). After correction, the model was able to predict calcium behavior very well ($R^2 = 0.980$).

4.2.3. Metals behavior in case 2-2 and case 2-3

To clarify the behavior of metals with the actual inlet concentrations of the P-cry unit in the advanced SRPR process, the thermodynamic calculation was carried out using actual inflow metal concentrations and initial phosphate concentration of 20 mg-P·L^{-1} for both batch tests (case 2-2 and case 2-3).

Calculation results of the precipitated metals with different molar ratios of Ca/P and a pH of 9.0 (case 2-2) are compared with measured ones as shown in Figure 6(a). The behaviors of potassium, barium, magnesium, calcium, chrome, manganese, and aluminum in measured results were in accordance with those calculated, while those for four other metals were different.

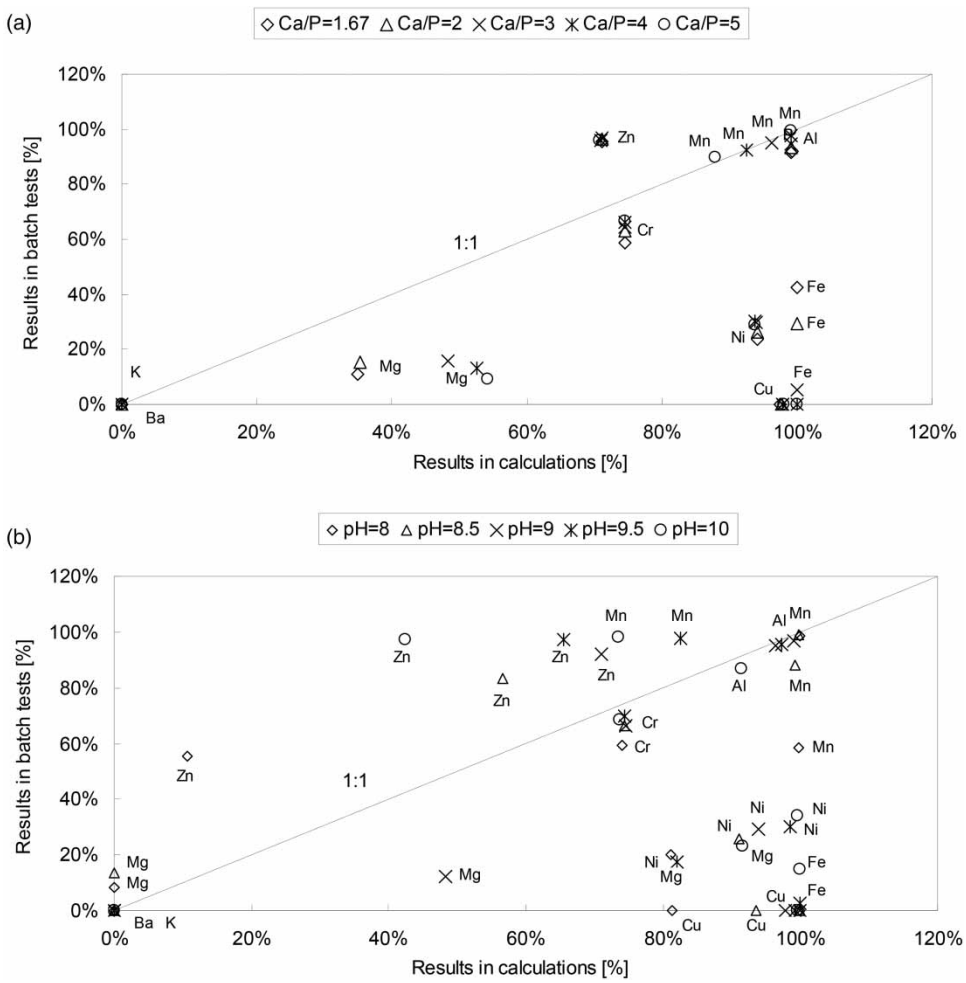

Figure 6 | Comparison of precipitated ratio of metals between calculated and measured results: (a) case 2-2 and (b) case 2-3.

Firstly, the behavior of iron, nickel, and copper was completely different: the measured results showed low precipitation only, while the calculation one achieved almost 100%. The difference should be accounted for by the slow generation rate of the corresponding precipitates. Secondly, about 70% of zinc was precipitated according to the calculation results and more than 95% for measured ones, which could not be explained by thermodynamics.

The comparison of the precipitation ratios of metals between measured results and those of thermodynamic calculation with different pH and molar ratio of Ca/P of 3.0 in case 2-3 is shown in Figure 6(b), which was similar to that in Figure 6(a). These results showed the limitation of thermodynamic modeling that should be paid attention to for the actual application of thermodynamic modeling.

4.3. Application of thermodynamic modeling

Thermodynamic modeling results showed that not only phosphorus recovery efficiency but also recovered product purity depends on the operational conditions (pH and molar Ca/P). In case 2-2, increased initial calcium concentration contributed to the generation of huntite and other precipitates under the calculation conditions, which led to the increased amount of impurity (co-precipitated solid besides for ACP and DHCP) with an elevated Ca/P molar ratio (Supplementary material, Figure S4(a)). In case 2-3, when pH was more than 8.5, the amount of impurity significantly increased as pH level rose, resulting in a clear decrease of the P ratio in the recovered product (Supplementary material, Figure S4(b)).

In the application of the modified thermodynamic model, the phosphorus recovery efficiency and behavior of metals as well as their effects on the quality or purity of recovered product with a pH of 8–10 and a Ca/P molar ratio of 1.67–5 were predicted. Thermodynamic calculation results indicated that more than 90% of phosphorus could be recovered under any of the following conditions: $pH = 8.5$ and $Ca/P \geq 4$ or $pH = 9$ and $Ca/P \geq 3$ or $pH = 9.5$ and $Ca/P \geq 2$ (Supplementary material, Figure S5(a)). However, with the increase of pH and molar ratio of Ca/P, the percentage of recovered phosphorus in the product decreased from about 20 to 10% (Supplementary material, Figure S5(b)), since the amount of impurity very noticeably increased from about 2 to 70 mg/L (Supplementary material, Figure S5(c)).

Phosphorus contents in the recovered product clearly decreased as both pH and the molar ratio of Ca/P increased. Thus, an overly high pH or molar ratio of Ca/P should be avoided considering the generation of impurity or the co-precipitation of metals. On the other hand, a pH of 9.0 and a Ca/P molar ratio of 3.0 were essential operational conditions for a recovery rate of more than 80% phosphorus according to experimental results (Supplementary material, Figure S2 and Figure 2). From the perspective of maximizing both phosphorus recovery efficiency and the quality or purity of recovered product, a pH of 9.0 and a Ca/P molar ratio of 3.0 were found to be the optimized operational conditions for phosphorus recovery with calcium phosphates in the advanced SRPR process where the content of the influent metal was at the level of actual municipal sewage.

5. CONCLUSIONS

In this study, phosphorus recovery by calcium phosphate and behaviors of metals were simulated by a modified thermodynamic model, in which precipitated phosphate and calcium were modified by incorporating correction equations, and the precipitated product was assumed to be ACP and DCPD only to simulate the short-term precipitation of calcium phosphates based on the experimental results and literature review. The modified thermodynamic model was verified with the experimental results of both batch tests and continuous experiments. Finally, phosphorus recovery and the behavior of metals were predicted by the modified thermodynamic model for the actual application of advanced sewage treatment process. The following main results are obtained:

- Batch experimental results indicated that phosphorus recovery efficiency decreased with the increase in metal content and more than 80% phosphorus can be recovered with a Ca/P molar ratio of 3.0 and a pH of 9.0 for SAT containing a high metal level.
- According to measured calcium and phosphate precipitation ratios, it was confirmed that HAP was not the main product in recovered phosphate, while the mixture of ACP and DCPD had a high possibility.
- A precipitated molar ratio of Ca/P in the recovered product was augmented with an increase in the initial Ca/P molar ratio or pH. Correspondingly, the ACP ratio in the recovered product increased while the DCPD decreased.
- ACP generation without the negative effect of other metals and carbonate in case 1 was more than that with metals and carbonate existing in case 2.

- The precipitated metal content, i.e., the impurity in the recovered product, clearly increased with an increase in both pH and the molar ratio of Ca/P for SAT with high metal contents.
- According to experimental results, the following correction equations were proposed with R^2 of 0.900 for phosphorus recovery rate and 0.980 for calcium precipitation rate.

$$K_{dev,P} = e^{-12.91} \cdot [pH]^{5.50} \cdot [Ca/P]_{init}^{0.51} \quad (\text{pH} < 9.0 \text{ or } [\text{Ca/P}]_{\text{init}} < 3.0)$$

$$R_{pred,P} = R_{thermo,P} \cdot K_{dev,P} \quad (\text{pH} < 9.0 \text{ or } [\text{Ca/P}]_{\text{init}} < 3.0)$$

$$R_{pred,Ca} = R_{thermo,Ca} \cdot K_{dev,P} \cdot (1 - C_{DCPD}/3) \quad (\text{pH} < 9.0 \text{ or } [\text{Ca/P}]_{\text{init}} < 3.0)$$

From the perspective of maximizing both the efficiency of phosphorus recovery and elevated quality or purity of recovered product, co-precipitation of metals should be controlled at a low level, it was concluded that a pH of 9.0 and a Ca/P molar ratio of 3.0 were the optimized operational conditions for phosphorus recovery with calcium phosphates in the advanced SRPR process where the content of the influent metal was at the level of actual municipal sewage.

ACKNOWLEDGEMENT

This work was supervised by Prof. Hiroshi TUSNO in Lake Biwa Environmental Research Institute and Prof. Hideaki NAGARE in Okayama University.

DATA AVAILABILITY STATEMENT

All relevant data are included in the paper or its Supplementary Information.

CONFLICT OF INTEREST

The authors declare there is no conflict.

REFERENCES

Allison, J. D., Brown, D. S. & Novo-Gradac, K. J. 1991 *MINTEQA2/PRODEFA2, A Geochemical Assessment Model for Environmental Systems: Version 3.0 User's Manual*. U.S. EPA, Athens, GA, USA.

Asai, T., Kaneko, T., Sega, K. & Kato, M. 2005 The fate of trace elements at sewage treatment plants in Nagoya city. *Journal of Japan Sewage Works Association* **42** (508), 85–95.

Barat, R., Montoya, T., Borras, L., Ferrer, J. & Seco, A. 2008 Interactions between calcium precipitation and the polyphosphate-accumulating bacteria metabolism. *Water Research* **42** (13), 3415–3424.

Battistoni, P., Fava, G., Pavan, P., Musacco, A. & Cecchi, F. 1997 Phosphate removal in anaerobic liquors by struvite crystallization without addition of chemicals: preliminary results. *Water Research* **31** (11), 2925–2929.

Boniardi, G., Turolla, A., Fiameni, L., Gelmi, E., Malpei, F., Bontempi, E. & Canziani, R. 2021 Assessment of a simple and replicable procedure for selective phosphorus recovery from sewage sludge ashes by wet chemical extraction and precipitation. *Chemosphere* **285**, 131476.

Cao, X. D. & Harris, W. 2008 Carbonate and magnesium interactive effect on calcium phosphate precipitation. *Environmental Science & Technology* **42** (2), 436–442.

Celen, I., Buchanan, J. R., Burns, R. T., Robinson, R. B. & Raman, D. R. 2007 Using a chemical equilibrium model to predict amendments required to precipitate phosphorus as struvite in liquid swine manure. *Water Research* **41** (8), 1689–1696.

Cieślik, B. & Konieczka, P. 2017 A review of phosphorus recovery methods at various steps of wastewater treatment and sewage sludge management. The concept of 'no solid waste generation' and analytical methods. *Journal of Cleaner Production* **142**, 1728–1740.

Cornel, P. & Schaum, C. 2009 Phosphorus recovery from wastewater: needs, technologies and costs. *Water Science and Technology* **59** (6), 1069–1076.

Dai, J., Tang, W.-T., Zheng, Y.-S., Mackey, H. R., Chui, H. K., van Loosdrecht, M. C. M. & Chen, G.-H. 2014 An exploratory study on seawater-catalysed urine phosphorus recovery (SUPR). *Water Research* **66**, 75–84.

Ferguson, J. F. & McCarty, P. L. 1971 Effects of carbonate and magnesium on calcium phosphate precipitation. *Environmental Science & Technology* **5** (6), 534–540.

Galey, B., Gautier, M., Kim, B., Blanc, D., Chatain, V., Ducom, G., Dumont, N. & Gourdon, R. 2022 Trace metal elements vaporization and phosphorus recovery during sewage sludge thermochemical treatment – a review. *Journal of Hazardous Materials* **424** (Part B), 127360.

Guedes, P., Couto, N., Ottosen, L. M. & Ribeiro, A. B. 2014 Phosphorus recovery from sewage sludge ash through an electrodialytic process. *Waste Management* **34** (5), 886–892.

Guney, K., Weidelener, A. & Krampe, J. 2008 Phosphorus recovery from digested sewage sludge as MAP by the help of metal ion separation. *Water Research* **42** (18), 4692–4698.
Jang, H. & Kang, S. H. 2002 Phosphorus removal using cow bone in hydroxyapatite crystallization. *Water Research* **36** (5), 1324–1330.
Keller, A., Burger, J., Steinmetz, H., Hasse, H. & Kohns, M. 2022 Thermodynamic modeling of phosphorus recovery from wastewater. *Waste and Biomass Valorization* **13** (6), 3013–3023.
Mamais, D., Pitt, P. A., Cheng, Y. W., Loiacono, J. & Jenkins, D. 1994 Determination of ferric-chloride dose to control struvite precipitation in anaerobic sludge digesters. *Water Environment Research* **66** (7), 912–918.
Maurer, M., Abramovich, D., Siegrist, H. & Gujer, W. 1999 Kinetics of biologically induced phosphorus precipitation in waste-water treatment. *Water Research* **33** (2), 484–493.
Meng, X., Huang, Q., Xu, J., Gao, H. & Yan, J. 2019 A review of phosphorus recovery from different thermal treatment products of sewage sludge. *Waste Disposal & Sustainable Energy* **1** (2), 99–115.
Meyer, H. J. 1984 The influence of impurities on the growth-rate of calcite. *Journal of Crystal Growth* **66** (3), 639–646.
Musvoto, E. V., Wentzel, M. C. & Ekama, G. A. 2000a Integrated chemical-physical processes modelling – II. Simulating aeration treatment of anaerobic digester supernatants. *Water Research* **34** (6), 1868–1880.
Musvoto, E. V., Wentzel, M. C., Loewenthal, R. E. & Ekama, G. A. 2000b Integrated chemical-physical processes modelling – I. Development of a kinetic-based model for mixed weak acid/base systems. *Water Research* **34** (6), 1857–1867.
Nagare, H., Tsuno, H., Saktaywin, W. & Soyama, T. 2008 Sludge ozonation and its application to a new advanced wastewater treatment process with sludge disintegration. *Ozone-Science & Engineering* **30** (2), 136–144.
Ovsyannikova, E., Arauzo, P. J., Becker, G. C & Kruse, A. 2019 Experimental and thermodynamic studies of phosphate behavior during the hydrothermal carbonization of sewage sludge. *Science of the Total Environment* **692**, 147–156.
Peng, L., Dai, H., Wu, Y., Peng, Y. & Lu, X. 2018a A comprehensive review of phosphorus recovery from wastewater by crystallization processes. *Chemosphere* **197**, 768–781.
Peng, L., Dai, H., Wu, Y., Peng, Y. & Lu, X. 2018b A comprehensive review of the available media and approaches for phosphorus recovery from wastewater. *Water, Air, & Soil Pollution* **229** (4), 115.
Pindine, G., Ojoawo, B. I., Trembly, J. & Daramola, D. 2021 Thermodynamic modeling of phosphorus recovery from wastewater for process optimization. *ECS Meeting Abstracts* **MA2021-01** (45), 1798.
Qiang, Z., Wang, L., Dong, H. & Qu, J. 2015 Operation performance of an A/A/O process coupled with excess sludge ozonation and phosphorus recovery: a pilot-scale study. *Chemical Engineering Journal* **268** (0), 162–169.
Qin, Y., Li, H., Ma, S., Li, K., Zhang, X., Hou, D., Zheng, X., Wang, C., Lyu, P., Xu, S. & Zhang, W. 2022 Recovery and utilization of phosphorus from fruit and vegetable wastewater. *Scientific Reports* **12** (1), 617.
Rootare, H. M., Deitz, V. R. & Carpenter, F. G. 1962 Solubility product phenomena in hydroxyapatite-water systems. *Journal of Colloid Science* **17** (3), 179–206.
Saktaywin, W., Tsuno, H., Nagare, H., Soyama, T. & Weerapakkaroon, J. 2005 Advanced sewage treatment process with excess sludge reduction and phosphorus recovery. *Water Research* **39** (5), 902–910.
Saktaywin, W., Tsuno, H., Nagare, H. & Soyarna, T. 2006 Operation of a new sewage treatment process with technologies of excess sludge reduction and phosphorus recovery. *Water Science and Technology* **53** (12), 217–227.
Salimi, M. H., Heughebaert, J. C. & Nancollas, G. H. 1985 Crystal-growth of calcium phosphates in the presence of magnesium-ions. *Langmuir* **1** (1), 119–122.
Schütte, T., Niewersch, C., Wintgens, T. & Yüce, S. 2015 Phosphorus recovery from sewage sludge by nanofiltration in diafiltration mode. *Journal of Membrane Science* **480**, 74–82.
Seckler, M. M., Bruinsma, O. S. L. & VanRosmalen, G. M. 1996 Calcium phosphate precipitation in a fluidized bed in relation to process conditions: a black box approach. *Water Research* **30** (7), 1677–1685.
Shaddel, S., Grini, T., Ucar, S., Azrague, K., Andreassen, J. P. & Osterhus, S. W. 2020 Struvite crystallization by using raw seawater: improving economics and environmental footprint while maintaining phosphorus recovery and product quality. *Water Research* **173**, 115572.
Song, Y., Hahn, H. H. & Hoffmann, E. 2002a The effect of carbonate on the precipitation of calcium phosphate. *Environmental Technology* **23** (2), 207–215.
Song, Y. H., Hahn, H. H. & Hoffmann, E. 2002b Effects of solution conditions on the precipitation of phosphate for recovery – a thermodynamic evaluation. *Chemosphere* **48** (10), 1029–1034.
Song, Y., Qian, F., Gao, Y., Huang, X., Wu, J. & Yu, H. 2015 PHREEQC program-based simulation of magnesium phosphates crystallization for phosphorus recovery. *Environmental Earth Sciences* **73** (9), 5075–5084.
Steen, I. 1998 Phosphorus availability in the 21st century: management of a non-renewable resource. *Phosphorus and Potassium* **217**, 25.
Tsuno, H., Arakawa, K., Kato, Y. & Nagare, H. 2008 Advanced sewage treatment with ozone under excess sludge reduction, disinfection and removal of EDCs. *Ozone-Science & Engineering* **30** (3), 238–245.
Wang, J. S., Song, Y. H., Yuan, P., Peng, J. F. & Fan, M. H. 2006 Modeling the crystallization of magnesium ammonium phosphate for phosphorus recovery. *Chemosphere* **65** (7), 1182–1187.
Yu, B., Xiao, X., Wang, J., Hong, M., Deng, C., Li, Y.-Y. & Liu, J. 2021 Enhancing phosphorus recovery from sewage sludge using anaerobic-based processes: current status and perspectives. *Bioresource Technology* **341**, 125899.

Yuan, Z., Pratt, S. & Batstone, D. J. 2012 Phosphorus recovery from wastewater through microbial processes. *Current Opinion in Biotechnology* **23** (6), 878–883.

Zhang, T., Ding, L. L., Ren, H. Q., Guo, Z. T. & Tan, J. 2010 Thermodynamic modeling of ferric phosphate precipitation for phosphorus removal and recovery from wastewater. *Journal of Hazardous Materials* **176** (1–3), 444–450.

Zhou, J., Pan, Y., Feng, X., Huang, Y. & Li, D.-P. 2022 Phosphorus recovery from biofilm-enriched sewage by fluidized bed crystallization of vivianite. *Journal of Environmental Chemical Engineering* **10** (3), 107800.

First received 15 January 2023; accepted in revised form 15 May 2023. Available online 25 May 2023